Isotopic composition of stratospheric water vapor: Measurements and photochemistry

David G. Johnson,[1] Kenneth W. Jucks, Wesley A. Traub, and Kelly V. Chance
Harvard-Smithsonian Center for Astrophysics, Cambridge, Massachusetts

Abstract

We present a photochemical model describing the changes in the isotopic composition of stratospheric water vapor that result from methane oxidation and reactions with O(^1D). We then compare model calculations with measurements made with the Smithsonian Astrophysical Observatory far-infrared spectrometer during seven balloon flights that took place between 1989 and 1997. The agreement between the model calculations and measurements establishes the validity of the model and the internal consistency of the data set. Finally, we use the model and measurements together to estimate the mixing ratio and isotopic composition of water vapor entering the stratosphere and find that the average over all flights of the water vapor mixing ratio, δD, δ^{18}O, and δ^{17}O are 3.48 ± 0.15 parts per million by volume, -679 ± 20‰, -128 ± 31‰, and -84 ± 31‰, respectively, where the errors indicate the estimated accuracy.

[1] Now at NASA Langley Research Center, Hampton, Virginia.

1. Introduction

Measurements of isotopic composition have been used to test photochemical models and quantify sources of several atmospheric trace gases [*Thiemens*, 1999, *Kaye*, 1987]. Isotope effects are especially large for water vapor in the atmosphere of the Earth, because much of the troposphere is near saturation, the saturation vapor pressure changes by > 3 orders of magnitude between the surface and the tropopause, and isotopically heavy water is preferentially removed during condensation. Simple models predict that if the tropospheric water vapor mixing ratio is reduced to stratospheric values, then the relative abundance of HDO should be depleted by $> 80\%$ relative to ocean water, although the observed depletion is closer to 67% [*Moyer et al.*, 1996]. The sensitivity of water vapor isotope ratios to processes occurring in the troposphere make such measurements useful for testing models of dehydration in the upper troposphere and stratosphere [*Johnson et al.*, this issue].

In the following sections we describe a photochemical model of the evolution of water vapor isotope ratios in the stratosphere. We then present observations of $H_2{}^{16}O$, $H_2{}^{17}O$, $H_2{}^{18}O$, and HDO made with the Smithsonian Astrophysical Observatory far-infrared spectrometer (FIRS-2). The observations are compared with model calculations to test both the model and the internal consistency of the measurements. Finally, we use the model and measurements together to estimate the initial volume mixing ratio and isotopic composition of water vapor in air entering the stratosphere.

2. Isotopic Standards

Measurements of an isotopic ratio R, such as $R = [\mathrm{HDO}]/[\mathrm{H_2O}]$, where $[X]$ signifies the volume mixing ratio of X, are typically reported relative to a standard ratio R_0, often using δ notation:

$$\delta(‰) \equiv 1000(R/R_0 - 1)\,.$$

We use the isotopic composition of standard mean ocean water as the standard and adopt the values 2.0052×10^{-3}, 3.7297×10^{-4}, and 1.5576×10^{-4} for $[^{18}\mathrm{O}]/[^{16}\mathrm{O}]$, $[^{17}\mathrm{O}]/[^{16}\mathrm{O}]$, and $[\mathrm{D}]/[\mathrm{H}]$, respectively [*De Bièvre et al.*, 1984]. When calculating δ, we assume standard ratios of $2(1.5576\times10^{-4})$ and $4(1.5576\times10^{-4})$ for $[\mathrm{HDO}]/[\mathrm{H_2O}]$ and $[\mathrm{CH_3D}]/[\mathrm{CH_4}]$, respectively.

In this paper we will consider only singly substituted isotopomers, since the natural abundance of H_2O molecules with multiple isotope substitutions is low enough to be ignored in the present discussion. In the following sections we will use Q to signify either $^{17}\mathrm{O}$ or $^{18}\mathrm{O}$ and O to signify $^{16}\mathrm{O}$.

3. Photochemistry of Water Vapor

Once air enters the stratosphere, the abundance of H_2O increases through the oxidation of methane, producing roughly two molecules of H_2O for each molecule of CH_4 destroyed [*Remsberg et al.*, 1996, *Abbas et al.*, 1996, *Dessler et al.*, 1994]. The isotopic composition of photochemically produced H_2O is determined by the $[\mathrm{D}]/[\mathrm{H}]$ ratio of methane and the $[\mathrm{Q}]/[\mathrm{O}]$ ratio of the oxygen reservoir. Isotope exchange between water and molecular hydrogen (H_2 and HD) has a negligible effect below 32 km [*Irion et al.*, 1996] and will not be considered here. The $[\mathrm{Q}]/[\mathrm{O}]$ ratio of stratospheric water vapor is also affected by O-atom exchange with the oxygen reservoir, initiated by the reaction with $\mathrm{O}(^1D)$ as described below.

The oxidation of methane is initiated primarily by the reactions

$$\mathrm{CH_4 + O(^1}D) \rightarrow \mathrm{CH_3 + OH}\,, \tag{1}$$

$$\mathrm{CH_4 + OH \rightarrow CH_3 + H_2O}\,, \tag{2}$$

$$\mathrm{CH_4 + Cl \rightarrow CH_3 + HCl}\,; \tag{3}$$

followed by rapid oxidation of CH_3 [*Lary and Tuomi*, 1997], leading to net production of $2H_2O + CO_2$. The oxidation of CH_3D is initiated by an analogous set of reactions, leading to net production of $HDO + H_2O + CO_2$ [*Irion et al.*, 1996].

Water vapor is destroyed primarily by the reaction

$$\mathrm{H_2O + O(^1}D) \rightarrow \mathrm{2OH}\,, \tag{4}$$

but loss of H_2O is temporary in the stratosphere. H_2O is regenerated through the reaction

$$\mathrm{OH + HO_2 \rightarrow H_2O + O_2}\,, \tag{5}$$

as well as by other reactions such as $\mathrm{OH + HNO_3}$, all of which terminate the HO_x catalytic cycle. For H_2O the cycle is equivalent to the following reaction:

$$\mathrm{H_2O^* + (O_2, O_3) \rightarrow H_2O + (OO^*, OOO^*)}\,, \tag{6}$$

where O^* indicates an oxygen atom that entered the stratosphere as part of a water molecule and the notation $(\mathrm{O_2, O_3})$ indicates that the oxygen reservoir is some combination of O_2 and O_3. The effective rate of reaction (6) is given by

$$d[\mathrm{H_2O^*}]/dt = -k_4 n[\mathrm{H_2O^*}][\mathrm{O(^1}D)]\,, \tag{7}$$

where k_4 is the rate constant for reaction (4) (the rate-limiting step for the cycle described by reactions (4) and (5)) and n is the molecule number density.

The rate of H_2O production by methane oxidation is given by twice the sum of the rate-limiting reactions (1)–(3), or

$$d[\mathrm{H_2O}]/dt = 2n[\mathrm{CH_4}](k_1[\mathrm{O}(^1D)] + k_2[\mathrm{OH}] + k_3[\mathrm{Cl}]) , \quad (8)$$

where k_1, k_2, and k_3 are the rate constants for reactions (1), (2), and (3), respectively. Similarly, the rate of HDO production by oxidation of CH_3D is given by

$$d[\mathrm{HDO}]/dt = n[\mathrm{CH_3D}](k_1'[\mathrm{O}(^1D)] + k_2'[\mathrm{OH}] + k_3'[\mathrm{Cl}]) , \quad (9)$$

where k_1', k_2', and k_3' are the rate constants for the deuterated versions of reactions (1), (2), and (3), respectively.

Oxygen exchange (reaction (6)) is both a source and a sink for H_2Q. We assume here that the rate constant for reaction (4) is the same for all oxygen isotopes, and that the oxygen isotope ratio for water produced in the stratosphere is given by the isotope ratio of the oxygen reservoir. In this case the rate of production of H_2Q by reaction (6) is $d[\mathrm{H_2Q}]/dt = -fd[\mathrm{H_2O^*}]/dt = fk_4n[\mathrm{H_2O^*}][\mathrm{O}(^1D)]$, where $f = [\mathrm{OQ}]/2[\mathrm{O_2}]$ if the oxygen reservoir is O_2, and $f = ([\mathrm{OOQ}]+[\mathrm{OQO}]+[\mathrm{QOO}])/3[\mathrm{O_3}]$ if the reservoir is O_3 (if the central oxygen atom does not participate in any reactions then $f = ([\mathrm{OOQ}]+[\mathrm{QOO}])/2[\mathrm{O_3}]$); and the rate of loss of H_2Q^* is $d[\mathrm{H_2Q^*}]/dt = -k_4n[\mathrm{H_2Q^*}][\mathrm{O}(^1D)]$. The net rate of change of H_2Q is given by the sum of the production and loss terms. Note that there is no net change if $[\mathrm{H_2Q^*}] = f[\mathrm{H_2O^*}]$.

The rate of production of H_2Q by methane oxidation is $d[\mathrm{H_2Q}]/dt = fd[\mathrm{H_2O}]/dt = 2fn[\mathrm{CH_4}](k_1[\mathrm{O}(^1D)] + k_2[\mathrm{OH}] + k_3[\mathrm{Cl}])$, where we have used (8) to substitute for $d[\mathrm{H_2O}]/dt$. After adding the effects of oxygen exchange and methane oxidation we derive the result

$$d[\mathrm{H_2Q}]/dt = 2fn[\mathrm{CH_4}](k_1[\mathrm{O}(^1D)] + k_2[\mathrm{OH}] + k_3[\mathrm{Cl}]) + fnk_4[\mathrm{H_2O^*}][\mathrm{O}(^1D)](1-[\mathrm{H_2Q^*}]/f[\mathrm{H_2O^*}]) . \quad (10)$$

Note that it follows from (7) and our earlier expression for $d[\mathrm{H_2Q^*}]/dt$ that $d([\mathrm{H_2Q^*}]/[\mathrm{H_2O^*}])/dt = 0$, and so $[\mathrm{H_2Q^*}]/[\mathrm{H_2O^*}] = [\mathrm{H_2Q}]_0/X_0$, where $[\mathrm{H_2Q}]_0$ and X_0 are the initial H_2Q and water vapor mixing ratios, respectively.

In the remainder of this section we integrate (8)–(10) and solve for the isotope ratios as functions of time. Finally, we show that the resulting expressions can be evaluated using a combination of measured quantities and model calculations.

We integrate (8) after making the substitution $d[\mathrm{H_2O}]/dt = -2d[\mathrm{CH_4}]/dt$ and derive the solution

$$[\mathrm{H_2O}] = X_0 + X_c , \quad (11)$$

where

$$X_c \equiv 2B_0[1 - \exp(-a_1 - a_2 - a_3)] , \quad (12)$$

B_0 is the initial methane mixing ratio, and

$$a_1(t) \equiv \int_0^t nk_1[\mathrm{O}(^1D)]d\tau , \quad (13)$$

$$a_2(t) \equiv \int_0^t nk_2[\mathrm{OH}]d\tau , \quad (14)$$

$$a_3(t) \equiv \int_0^t nk_3[\mathrm{Cl}]d\tau . \quad (15)$$

The integrals are along the air parcel trajectory. Note that X_c is simply the amount of water that has been produced through the oxidation of methane, and can be calculated from a measurement of the local methane mixing ratio and an estimate of B_0.

Similarly, we integrate (9) and derive the solution

$$[\mathrm{HDO}] = [\mathrm{HDO}]_0 + [\mathrm{CH_3D}]_0[1 - \exp(-a_1' - a_2' - a_3')] , \quad (16)$$

where $[\mathrm{HDO}]_0$ and $[\mathrm{CH_3D}]_0$ are the initial deuterated water and methane mixing ratios, respectively; and a_1', a_2', and a_3' are given by (13)–(15) after replacing k_1–k_3 with k_1'–k_3'.

We integrate (10) by substituting $fd[\mathrm{H_2O}]/dt$ (from (8)) for the first term in (10) and $-f(1 - [\mathrm{H_2Q}]_0/fX_0)$ $d[\mathrm{H_2O^*}]/dt$ (from (7)) for the second term, and find that

$$[\mathrm{H_2Q}] = f[\mathrm{H_2O}] - f[\mathrm{H_2O^*}](1 - [\mathrm{H_2Q}]_0/fX_0) . \quad (17)$$

We integrate (7) to derive the solution

$$[\mathrm{H_2O^*}] = X_0 \exp(-a_4) , \quad (18)$$

where

$$a_4(t) \equiv \int_0^t nk_4[\mathrm{O}(^1D)]d\tau . \quad (19)$$

By combining (11)–(12) and (17)–(18), we derive the result

$$[\mathrm{H_2Q}] = 2fB_0[1 - \exp(-a_1 - a_2 - a_3)] + fX_0[1 - (1 - [\mathrm{H_2Q}]_0/fX_0)\exp(-a_4)] . \quad (20)$$

We now consider the ratios [HDO]/[H_2O] and [H_2Q]/[H_2O]. First, we derive the following relationships from (12):

$$\exp(-a_1 - a_2 - a_3) = 1 - X_c/2B_0 \,, \tag{21}$$

$$\exp(-a_1' - a_2' - a_2') = (1 - X_c/2B_0)^{\zeta(t)} \,, \tag{22}$$

$$\exp(-a_4) = (1 - X_c/2B_0)^{\xi(t)} \,; \tag{23}$$

where

$$\zeta(t) \equiv (a_1' + a_2' + a_3')/(a_1 + a_2 + a_3) \,, \tag{24}$$

$$\xi(t) \equiv a_4/(a_1 + a_2 + a_3) \,. \tag{25}$$

We derive the following solutions from (11), (16), and (20) using (21)–(23):

$$\frac{[\mathrm{HDO}]}{[\mathrm{H_2O}]} = \frac{[\mathrm{HDO}]_0}{X_0}\frac{X_0}{X_0 + X_c} + \frac{[\mathrm{CH_3D}]_0}{B_0}\frac{B_0}{X_0 + X_c}\left[1 - \left(1 - \frac{X_c}{2B_0}\right)^{\zeta(t)}\right] ,$$

$$\frac{[\mathrm{H_2Q}]}{[\mathrm{H_2O}]} = f + \frac{X_0}{X_0 + X_c}\left(\frac{[\mathrm{H_2Q}]_0}{X_0} - f\right)\left(1 - \frac{X_c}{2B_0}\right)^{\xi(t)} .$$

Equivalently, using the δ notation defined earlier, we have

$$\delta\mathrm{D} = \delta\mathrm{D}_0\frac{X_0}{X_0 + X_c} + \delta\mathrm{D}_m\frac{2B_0}{X_0 + X_c}\left[1 - \left(1 - \frac{X_c}{2B_0}\right)^{\zeta(t)}\right] + \frac{2000B_0}{X_0 + X_c}\left[\left(1 - \frac{X_c}{2B_0}\right) - \left(1 - \frac{X_c}{2B_0}\right)^{\zeta(t)}\right] , \tag{26}$$

$$\delta\mathrm{Q} = \delta\mathrm{Q}_r + (\delta\mathrm{Q}_0 - \delta\mathrm{Q}_r)\frac{X_0}{X_0 + X_c}\left(1 - \frac{X_c}{2B_0}\right)^{\xi(t)} ; \tag{27}$$

where δD and δQ are the observed isotopes ratios; $\delta\mathrm{D}_0$ and $\delta\mathrm{Q}_0$ are the starting ratios for water; $\delta\mathrm{D}_m$ is the starting isotope ratio for methane; and $\delta\mathrm{Q}_r = 1000(f/R_0 - 1)$. The factor of 2 appears in the last two terms of (26), because the standard ratio for [CH_3D]/[CH_4] is twice the standard ratio for [HDO]/[H_2O], as described in section 2..

Equations (26) and (27) express δD and δQ as functions of X_c, $\zeta(t)$, $\xi(t)$, and a set of initial conditions. We now derive approximate expressions for $\zeta(t)$ and $\xi(t)$ by following a procedure similar to that outlined by *Irion et al.* [1996]. First, we define the ratios $f_1 \equiv a_1/(a_1 + a_2 + a_3)$, $f_2 \equiv a_2/(a_1 + a_2 + a_3)$, $f_3 \equiv a_3/(a_1 + a_2 + a_3)$, $\gamma_1 \equiv a_1'/a_1$, $\gamma_2 \equiv a_2'/a_2$, $\gamma_3 \equiv a_3'/a_3$, and $\gamma_4 \equiv a_4'/a_1$. We take the following rate constants from *DeMore et al.* [1997], all in units of molecule $\mathrm{cm^3\,s^{-1}}$: $k_1 = 1.5 \times 10^{-10}$, $k_2 = 2.45 \times 10^{-12}\exp(-1775/\mathrm{T})$, $k_3 = 1.1 \times 10^{-11}\exp(-1400/\mathrm{T})$, $k_4 = 2.2 \times 10^{-10}$, $k_2' = 3.5 \times 10^{-12}\exp(-1950/\mathrm{T})$, and $k_3' = 0.74k_3$ (at 298 K). The rate constant for k_1' has not been reported, and we will assume that $k_1' = k_1$ [*Irion et al.*, 1996]. Since the ratios k_1'/k_1 and k_4/k_1 are constant, it follows from (13) and (19) that $\gamma_1 = k_1'/k_1 = 1$ and $\gamma_4 = k_4/k_1 = 1.47$. We further assume that $k_3'/k_3 = 0.74$ at all stratospheric temperatures and that $k_2'/k_2 = 0.668$ (it actually varies from 0.60 to 0.69 at temperatures between 200 and 240 K, which is a typical temperature range for the midlatitude stratosphere), so that $\gamma_2 = 0.668$ and $\gamma_3 = 0.74$. After making these substitutions in (24)–(25) we find that

$$\zeta(t) = \gamma_1 f_1 + \gamma_2 f_2 + \gamma_3 f_3 \,, \qquad \zeta(t) = f_1 + 0.668 f_2 + 0.74 f_3 \,; \tag{28}$$

$$\xi(t) = \gamma_4 f_1 \,, \qquad \xi(t) = 1.47 f_1 \,. \tag{29}$$

The ratios f_1, f_2, and f_3 correspond to the fraction of total oxidized methane that has reacted with O(^1D), OH, and Cl, respectively. We estimate these ratios (as functions of X_c rather than t) using the model results published by *Lary and Tuomi* [1997], adjusting their values slightly to force $f_1 + f_2 + f_3 = 1$. Errors in estimating f_1–f_3 will have a small effect on $\zeta(X_c)$, but may significantly affect our estimate of $\xi(X_c)$, and thus the oxygen results.

We assume constant values of 1.71 parts per million by volume (ppmv) and -71‰ for B_0 and $\delta\mathrm{D}_m$, respectively [*Dlugokencky et al.*, 1994, *Irion et al.*, 1996]. We further assume that oxygen is exchanged primarily with O_2 and not O_3 [*Kaye*, 1990], so that $\delta\mathrm{Q}_r$ is 23.5‰ and 12.2‰ for ^{18}O and ^{17}O, respectively [*Johnston and Thiemens*, 1997, *Kroopnick and Craig*, 1972].

We can use (26)–(27) to calculate δD and δQ as functions of X_c once we determine X_0, $\delta\mathrm{D}_0$, and $\delta\mathrm{Q}_0$. We can also use the same relations to estimate X_0, $\delta\mathrm{D}_0$, and $\delta\mathrm{Q}_0$ from measurements of [H_2O], δD, δQ, and [CH_4]. We do both in section 5..

4. Measurements

The FIRS-2 is a remote-sensing Fourier transform spectrometer that observes the thermal emission of the atmosphere from balloon and aircraft platforms [*Johnson et al.*, 1995]. The spectral range was limited to 80–700 $\mathrm{cm^{-1}}$

until 1996, when we extended the high-frequency limit to 1250 cm^{-1} by improving the beamsplitter design [*Dobrowolski and Traub*, 1996]. During our most recent balloon flight the increased spectral range allowed us to measure vertical profiles for temperature, pressure, and the mixing ratio of 25 different molecules. The data considered here were obtained during six balloon flights that took place between 1989 and 1994 at latitudes near 33°N, in addition to a single 1997 balloon flight at a latitude of 68°N.

The unapodized spectrometer resolution of 0.004 cm^{-1} is sufficient to resolve many individual rotational transitions for [$H_2{}^{16}O$], [$H_2{}^{17}O$], [$H_2{}^{18}O$], and [HDO]. For each species we carefully select a number of fitting windows that contain unsaturated rotational transitions (intensity $< 5 \times 10^{-22}$ cm after adjusting for the relative isotopic abundance) with low ground state energies (< 1700 cm^{-1}) in order to minimize systematic errors. We also reject any lines that contribute $< 90\%$ to the optical depth of an unresolved feature. We find 18, 26, 11, and 32 transitions within our spectral bands that meet these criteria for $H_2{}^{16}O$, HDO, $H_2{}^{17}O$, and $H_2{}^{18}O$, respectively. Only 15 of the selected HDO transitions occur in regions of FIRS-2 spectra that had useful sensitivity before 1997.

Our initial analysis was based on line parameters from HITRAN92 [*Rothman et al.*, 1992] with the following modifications: line positions for H_2O and H_2Q are taken from *Toth* [1991, 1992], and HDO strengths and positions are taken from the Jet Propulsion Laboratory (JPL) submillimeter line catalog [*Poynter and Pickett*, 1984] for lines below 334 cm^{-1}. The large difference between the observed H_2O and H_2Q line positions and the calculated positions in HITRAN92 suggests that there may also be large errors in the calculated HITRAN92 strengths. In the past 2 years we have received improved calculations for $H_2{}^{16}O$ [*Coudert*, 1999] and $H_2{}^{18}O$ (J. C. Pearson, personal communication, 2000) and have calculated strengths and positions for $H_2{}^{17}O$ using the SPFIT and SPCAT routines from JPL [*Pickett*, 1991]. The new calculations provide greatly improved line positions and confirm that the strengths listed in HITRAN92 for the transitions meeting our selection criteria have errors as large as 25%. All FIRS-2 measurements presented here are based on the improved calculations. We estimate that average systematic errors due to uncertainty in the calculated strengths are $< 3\%$ for all isotopic variants, although errors in individual lines may still be as large as 25%. Previous analyses of FIRS-2 data are based on retrievals using the HITRAN92 strengths [*Keith*, 2000, *Dessler*, 1998], and so the measurements discussed in earlier publications differ from those presented here, although we note that the difference is less than the estimated systematic errors.

We present FIRS-2 measurements of [H_2O], δD, $\delta^{18}O$, and $\delta^{17}O$ in Figure 1. Average profiles for each flight are shown together with the estimated precision (1 standard deviation) for selected profiles and a weighted average over all flights. Data are weighted by the reciprocal of the variance when calculating the average. Also shown are average profiles measured by Atmospheric Trace Molecule Spectroscopy (ATMOS) [*Rinsland et al.*, 1991]. The FIRS-2 results are consistent with ATMOS measurements, except that FIRS-2 measurements show rapidly increasing depletions in $H_2{}^{17}O$ below 25 km that are not reflected in the ATMOS data. We believe that these large depletions are indicative of increasing systematic errors at low altitude, as discussed in the next section. More recent ATMOS measurements and analyses of δD (but not $\delta^{18}O$ or $\delta^{17}O$) are available [*Irion et al.*, 1996, *Moyer et al.*, 1996] and will also be discussed in the next section. In general, air in the lower stratosphere is dry and depleted in the heavy isotopes. Water vapor increases in abundance and becomes less depleted in heavy isotopes as the altitude increases.

5. Comparison With Model

In this section we first use a model to test for self-consistency in our measurements of $\delta^{17}O$ and $\delta^{18}O$. We then use our measurements of $\delta^{18}O$ and δD to test the photochemical model we developed in section 3.. Finally, we use the model to correct for photochemical aging and estimate the initial isotopic composition of stratospheric water vapor.

5.1. Measured $\delta^{17}O$ versus $\delta^{18}O$

Water vapor in the troposphere is depleted in heavy isotopes because of the vapor pressure isotope effect (VPIE); *Jancso and Van Hook* [1974] and *Kaye* [1987] provide comprehensive reviews of the subject. Kinetic effects contribute if the air is supersaturated [*Jouzel and Merlivat*, 1984] and are considered in a companion paper [*Johnson et al.*, this issue]. For saturated vapor in isotopic equilibrium with a condensed phase (liquid or solid), the isotope ratio in the vapor is proportional to the isotope ratio in the condensate. We define the isotopic fractionation factor $\alpha \equiv R_c/R_v$, where R_c is the isotope ratio ([H_2Q]/[H_2O] or [HDO]/[H_2O]) in the condensed phase and R_v is the ratio in the vapor phase. In general, α depends on temperature, the isotopes involved, and the phase of the condensate. However, the ratio $(\alpha_{17} - 1)/(\alpha_{18} - 1)$ (where α_{17} and α_{18} are the ratios for $H_2{}^{17}O$ and $H_2{}^{18}O$, respectively) is nearly constant. Model calculations by *Van Hook*

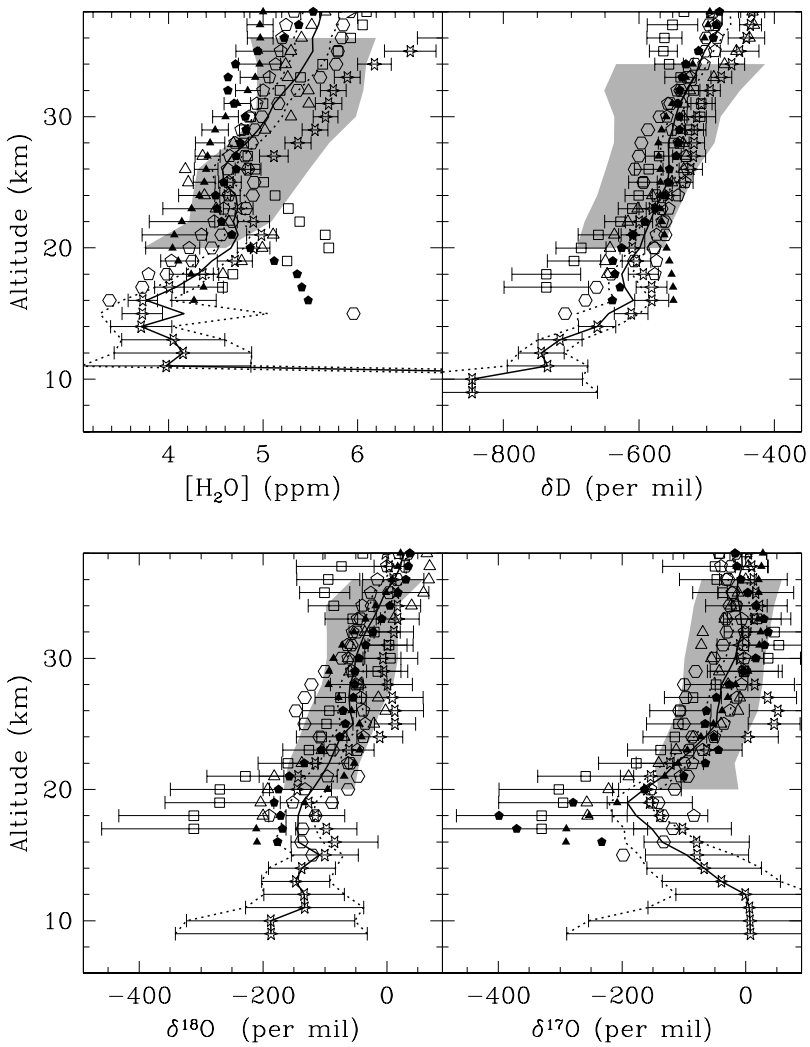

Figure 1. Measurements of [H_2O], δD, δ^{18}O, and δ^{17}O from seven balloon flights of the far-infrared spectrometer (FIRS-2). The launch dates are September 26, 1989 (solid triangles); June 4, 1990 (open triangles); May 29, 1992 (open squares); September 29, 1992 (solid pentagons); March 23, 1993 (open pentagons); May 22, 1994 (open hexagons); and April 30, 1997 (stars); error bars indicate estimated precision for representative profiles. Solid curves show the weighted average of all FIRS-2 profiles; 1σ error in the average is indicated by the dotted curve. The shaded area indicates average profiles from Atmospheric Trace Molecule Spectroscopy [*Rinsland et al.*, 1991]; the width shows the estimated 1σ precision.

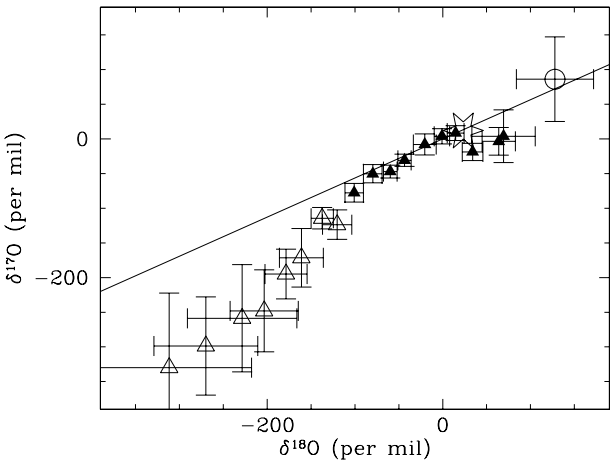

Figure 2. Three-isotope plot for water vapor. FIRS-2 measurements are binned by δ^{18}O and averaged. Open triangles indicate FIRS-2 measurements having an average altitude below 21 km, and solid triangles indicate measurements above. The open star indicates the isotopic composition of O_2 [*Kroopnick and Craig,* 1972, *Johnston and Thiemens,* 1997], and the open circle represents the FIRS-2 measurement of the isotopic composition of stratospheric O_3 [*Johnson et al.,* 2000]. We also show the depletion predicted from the vapor pressure isotope effect as a solid line with a slope of 0.564.

[1968] suggest that the ratio has the average value 0.529 and varies by 0.1% between 200 and 360 K. Measurements at temperatures between 313 and 363 K indicate that the ratio is independent of temperature but has the average value 0.564 rather than 0.529 [*Jancso and Van Hook,* 1974]. We adopt the value 0.564.

If air is dehydrated by continually condensing water vapor and removing the condensate to prevent further isotope exchange, it follows from conservation principles and the definition of α that $dR_v/R_v = (\alpha - 1)d[\mathrm{H_2O}]/[\mathrm{H_2O}]$ [*Smith,* 1992]. We use this and the definition of δ to derive the relation

$$d(\delta^{17}\mathrm{O})/d(\delta^{18}\mathrm{O}) = (1000 + \delta^{17}\mathrm{O})(\alpha_{17} - 1)/ (1000 + \delta^{18}\mathrm{O})(\alpha_{18} - 1)\,. \quad (30)$$

For modest depletions, $(1000+\delta^{17}\mathrm{O})/(1000+\delta^{18}\mathrm{O}) \approx 1$, and we estimate that $d(\delta^{17}\mathrm{O})/d(\delta^{18}\mathrm{O}) = 0.564$. The data above 21 km are in excellent agreement with this prediction, as shown in Figure 2. The data below 21 km indicate ^{17}O depletions $\sim$ 2 standard deviations larger than predicted. This is partially due to the fact that random errors in measured [H_2O] cause correlated errors in the calculated δ^{17}O and δ^{18}O that tend to distribute the measurements along a line with a slope of 1 rather than 0.564. We believe that the difference below 21 km also indicates that systematic errors increase at low altitude, possibly because saturation in the far-infrared increases the statistical weight of the midinfrared lines, and these lines may have different line parameter errors. Further improvements to the spectral line database are needed.

We also show in Figure 2 the isotopic composition of O_2 and FIRS-2 measurements of the composition of O_3 [*Johnson et al.,* 2000]; we note that other groups have observed enrichments in heavy ozone larger than those seen by FIRS-2 [*Mauersberger,* 1981, *Schueler et al.,* 1990]. The isotopic composition of H_2O appears to approach the composition of O_2, but because the isotopic compositions of both O_2 and O_3 lie on or near the relationship determined by the VPIE, we cannot establish the isotopic composition of the oxygen reservoir without sampling air that is old enough to be in isotopic equilibrium with the reservoir. We estimate that δQ retains 27% of the initial depletion for the oldest air observed by FIRS-2, so we cannot rule out the possibility that H_2O becomes enriched in heavy oxygen relative to O_2. On the basis of FIRS-2 measurements of the isotopic composition of O_3 and the results of models that indicate H_2O will show, at most, 23% of the isotopic enrichment seen in O_3 [*Kaye,* 1990; C. Bechtel and A. Zahn, The isotope composition of water vapor: A powerful tool to study transport and chemistry of middle atmospheric water vapor, submitted to *Journal of Geophysical Research,* 2000], we estimate that assuming O_2 is the reservoir results in a maximum error in estimating δQ_r of 24‰ and 17‰ for ^{18}O and ^{17}O, respectively.

We believe that the excellent agreement between predicted and measured δ^{17}O as a function of δ^{18}O indicates that the average systematic errors do not exceed 30‰ above 21 km.

5.2. Measured δD, δ^{18}O, and [H_2O]

In Figure 3 we compare measured δD and δ^{18}O as functions of [H_2O] with the result of calculations using (26)–(27), where $[\mathrm{H_2O}] = X_0 + X_c$ and we adopt values of 3.5 ppmv, -670‰, and -130‰ for X_0, $\delta\mathrm{D}_0$, and $\delta^{18}\mathrm{O}_0$, respectively. The observed δD shows good agreement with the results of (26), while the observed δ^{18}O differs significantly from the model. The fact that differences between observations and model have similar shapes for δD and δ^{18}O suggests that there may be systematic errors in average measured [H_2O] that vary by $\sim$ 3%, consistent with our earlier estimates. Changing [H_2O] by 3% changes a depletion of -670‰ by 10‰ but changes a depletion of -130‰ by 25‰, as indicated by the dashed

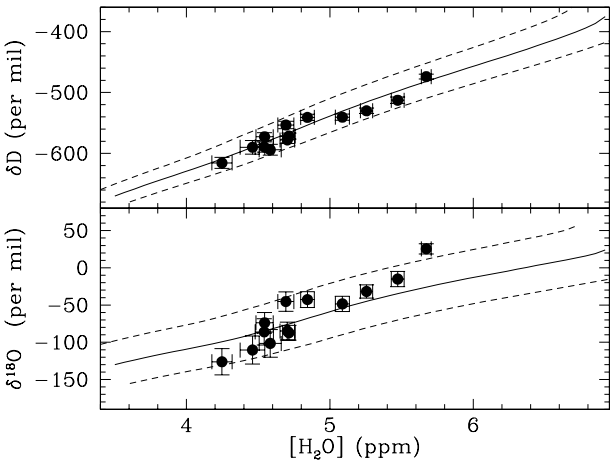

Figure 3. Comparison between measured and modeled δD and δ^{18}O. Data are averaged after binning by FIRS-2 measurements of [N_2O] (as a proxy for [CH_4]) to minimize effects of the correlation between errors in measured [H_2O] and δ. Solid curves show model calculations discussed in the text; effect of $\pm 3\%$ error in [H_2O] is indicated by the dashed curves.

curves in Figure 3.

5.3. Estimated δD_0, $\delta^{18}O_0$, and X_0

In order to use (26)–(27) to estimate δD_0 and $\delta^{18}O_0$, we require measurements of δD, δ^{18}O, [H_2O], and [CH_4]. FIRS-2 was unable to measure [CH_4] until 1997, and the 1997 measurements have relatively low precision. Because direct measurements are unavailable, we estimate [CH_4] from FIRS-2 measurements of [N_2O] and potential temperature using a relationship we derived from measurements made by the JPL MkIV interferometer [*Toon*, 1991, *Toon et al.*, 1992, *Johnson et al.*, 1999].

We show the results in Figure 4. The estimates of $\delta^{17}O_0$ and $\delta^{18}O_0$ become increasingly uncertain as the air ages, because the initial isotope ratio relaxes exponentially toward the isotope ratio of the oxygen reservoir (see (27)) and any knowledge of the initial isotope ratio is lost. The estimates of X_0 are quite variable in young air owing to the annual cycle propagating out of the tropics, and as described earlier, we believe that the measurements of δ^{17}O (and possibly δ^{18}O) are unreliable below 21 km. We average measurements in the middle of the range, defined as potential temperatures between 550 and 900 K, and estimate that average X_0, δD_0, $\delta^{18}O_0$, and $\delta^{17}O_0$ are 3.48 ± 0.15 ppmv, -679 ± 20‰, -128 ± 31‰, and -84 ± 31‰, respectively, where the errors indicate the estimated accuracy (1 standard deviation).

There have been many estimates of the initial water vapor mixing ratio in stratospheric air, and they are not consistent. Estimates fall between 2.7 and 4.1 ppmv, and the average over all estimates is 3.7 ppmv with a standard deviation of 0.25 [*Kley et al.*, 2000]. There are a number of reasons why the estimates may disagree, including instrumental errors, differences in sampling, and actual changes over time. A discussion of these differences is beyond the scope of this paper; *Kley et al.* [2000] provide a comprehensive review.

Our estimate of δD_0 agrees well with an earlier estimate of -670 ± 80‰ based on ATMOS measurements of [H_2O], [HDO], [CH_4], and [CH_3D] [*Moyer et al.*, 1996]. *Kaye* [1990] estimated that $\delta^{18}O_0$ would be in the range -50 to -100‰ if the tropospheric relationship between δD and δ^{18}O were valid for air entering the stratosphere, while we find somewhat larger depletions. Although other measurements of δ^{17}O are available [*Rinsland et al.*, 1991], we are not aware of any estimates other than those presented here of $\delta^{17}O_0$ in air reaching the midlatitude middle stratosphere.

6. Conclusion

We find good general agreement between FIRS-2 measurements of the isotopic composition of stratospheric water vapor and calculations with our photochemical model. The observed correlation between δ^{17}O and δ^{18}O agrees well with the model for measurements above 21 km, while the increasing effect of systematic errors (primarily spectroscopic) for measurements below 21 km result in differences between measurements and model of roughly 2 standard deviations. The observed correlation between δD and [H_2O] agrees well with the model, as does the average correlation between δ^{18}O and [H_2O], although the scatter in the measurements of δ^{18}O is larger than expected from the estimated precision. After using the model to remove the effects of photochemical aging from the measurements, we find that the average initial water vapor abundance and isotopic composition of air which crosses the tropopause and reaches the midlatitude middle stratosphere is given by $(X_0, \delta D_0, \delta^{18}O_0, \delta^{17}O_0) = (3.48 \pm 0.15$ ppmv$, -679 \pm 20$‰$, -128 \pm 31$‰$, -84 \pm 31$‰$)$, where the errors indicate the estimated accuracy (1 standard deviation). The significance of our results for understanding troposphere-stratosphere exchange and upper tropospheric humidity is discussed by *Johnson et al* [this issue].

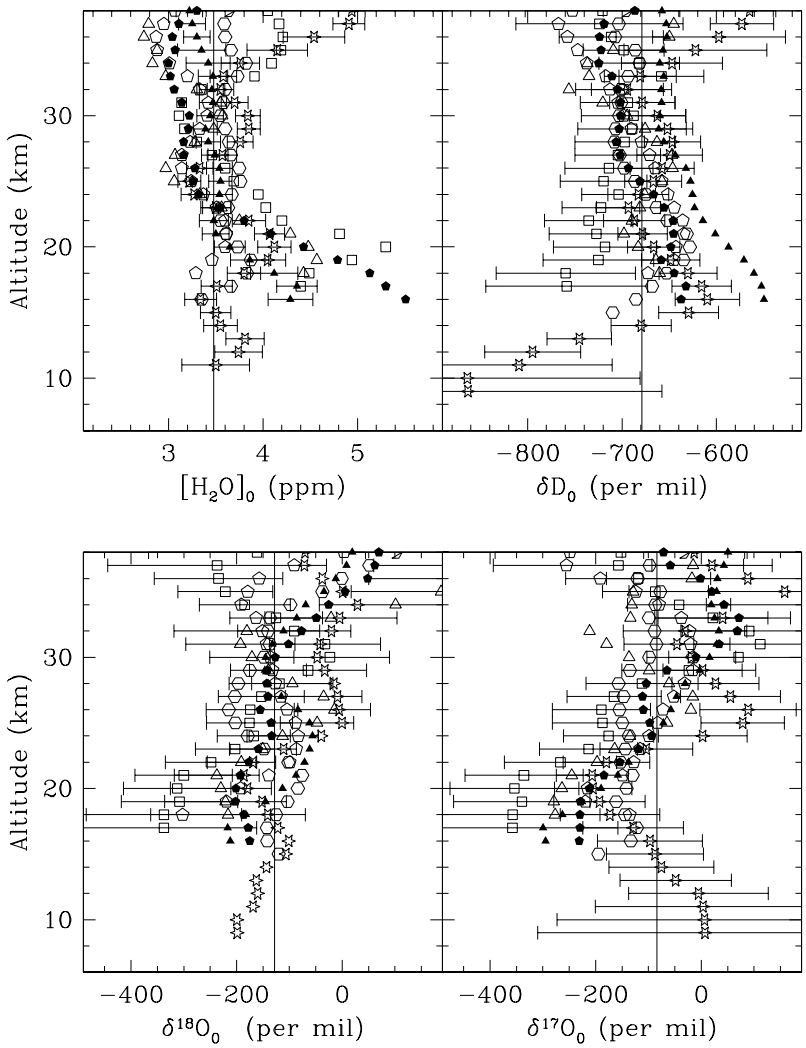

Figure 4. Measurements of $[H_2O]$, δD, δ^{18}O, and δ^{17}O from seven balloon flights of FIRS-2, after correcting for the effects of photochemical aging. The launch dates are September 26, 1989 (solid triangles); June 4, 1990 (open triangles); May 29, 1992 (open squares); September 29, 1992 (solid pentagons); March 23, 1993 (open pentagons); May 22, 1994 (open hexagons); and April 30, 1997 (stars); error bars indicate estimated precision for representative profiles. Vertical lines indicate average value for potential temperatures between 550 (23 km) and 900 K (32.5 km).

Acknowledgments We gratefully acknowledge support from NASA's Upper Atmosphere Research Program in the form of grants NSG 5175 and NAG5-8204. Technical assistance for the balloon flight was provided by the Jet Propulsion Laboratory and the National Scientific Balloon Facility. We thank Laurent Coudert for providing calculations, John Pearson for providing both calculations and advice, and Geoff Toon for providing MkIV measurements of [CH_4] and [N_2O].

References

Abbas, M. M., et al., The hydrogen budget of the stratosphere inferred from ATMOS measurements of H_2O and CH_4, *Geophys. Res. Lett.23,* 2405-2408, 1996.

Coudert, L. H., Line frequency and line intensity analyses of water vapour, *Mol. Phys., 96,* 941-954, 1999.

De Bièvre, P., M. Gallet, N. E. Holden, and I. L. Barnes, Isotopic abundances and atomic weights of the elements, *J. Phys. Chem. Ref. Data, 13,* 809-891, 1984.

DeMore, W. B., et al., Chemical kinetics and photochemical data for use in stratospheric modeling: Evaluation number 12, *JPL Publ., 97-4*, 1997.

Dessler, A. E., A reexamination of the "stratospheric fountain" hypothesis, *Geophys. Res. Lett.25,* 4165-4168, 1998.

Dessler, A. E., et al., An examination of the total hydrogen budget of the lower stratosphere, *Geophys. Res. Lett.21,* 2563-2566, 1994.

Dlugokencky, E. J., L. P. Steele, P. M. Lang, and K. A. Masarie, The growth rate and distribution of atmospheric methane, *J. Geophys. Res.99,* 17,021-17,043, 1994.

Dobrowolski, J. A., and W. A. Traub, New designs for far-infrared beamsplitters, *Appl. Opt., 35,* 2934-2946, 1996.

Irion, F. W. et al., Stratospheric observations of CH_3D and HDO from ATMOS Infrared Solar Spectra: Enrichments of deuterium in methane and implications for HD, *Geophys. Res. Lett.23,* 2381-2384, 1996.

Jancso, G., and W. A. Van Hook, Condensed phase isotope effects (especially vapor pressure isotope effects), *Chem. Rev. Washington D. C., 74,* 689-750, 1974.

Johnson, D. G., K. W. Jucks, W. A. Traub, and K. V. Chance, Smithsonian stratospheric far-infrared spectrometer and data reduction system, *J. Geophys. Res.100,* 3091-3106, 1995.

Johnson, D. G., K. W. Jucks, W. A. Traub, K. V. Chance, G. C. Toon, J. M. Russell III, and M. P. McCormick, Stratospheric age spectra derived from observations of water vapor and methane, *J. Geophys. Res.104,* 21,595-21,602, 1999.

Johnson, D. G., K. W. Jucks, W. A. Traub, and K. V. Chance, Isotopic composition of stratospheric ozone, *J. Geophys. Res.105,* 9025-9031, 2000.

Johnson, D. G., K. W. Jucks, W. A. Traub, and K. V. Chance, Isotopic composition of stratospheric water vapor: Implications for transport, *J. Geophys. Res.*this issue.

Johnston, J. C., and M. H. Thiemens, The isotopic composition of tropospheric ozone in three environments, *J. Geophys. Res.102,* 25,395-25,404, 1997.

Jouzel, J., and L. Merlivat, Deuterium and oxygen 18 in precipitation: Modeling of the isotopic effects during snow formation, *J. Geophys. Res.89,* 11,749-11,757, 1984.

Kaye, J. A., Mechanisms and observations for isotope fractionation of molecular species in planetary atmospheres, *Rev. Geophys., 25,* 1609-1658, 1987.

Kaye, J. A., Analysis of the origins and implications of the ^{18}O content of stratospheric water vapor, *J. Atmos. Chem., 10,* 39-57, 1990.

Keith, D. W., Stratosphere-troposphere exchange: Inferences from the isotopic composition of water vapor, *J. Geophys. Res.105,* 15,167-15,173, 2000.

Kley, D., et al., SPARC assessment of upper tropospheric and stratospheric water vapour, *Rep. 2,* Stratospheric Processes and Their Role in Climate, Paris, 2000.

Kroopnick, P., and H. Craig, Atmospheric oxygen: Isotopic composition and solubility fractionation, *Science, 175,* 54-55, 1972.

Lary, D. J., and R. Tuomi, Halogen-catalyzed methane oxidation, *J. Geophys. Res.102,* 23,421-23,428, 1997.

Mauersberger, K., Measurement of heavy ozone in the stratosphere, *Geophys. Res. Lett.8,* 935-937, 1981.

Moyer, E. J., F. W. Irion, Y. L. Yung, and M. R. Gunson, ATMOS stratospheric deuterated water and implications for troposphere-stratosphere transport, *Geophys. Res. Lett.23,* 2385-2388, 1996.

Pickett, H. M., The fitting and prediction of vibration-rotation spectra with spin interactions, *J. Mol. Spectrosc., 148,* 371-377, 1991.

Poynter, R. L., and H. M. Pickett, Submillimeter, millimeter, and microwave spectral line catalog, *Publ. 80-23,* rev. 2, Jet Propul. Lab., Pasadena, Calif., 1984.

Remsberg, E. E., P. P. Bhatt, and J. M. Russell III, Estimates of the water vapor budget of the stratosphere from UARS HALOE data, *J. Geophys. Res.101,* 6749-6766, 1996.

Rinsland, C. P., M. R. Gunson, J. C. Foster, R. A. Toth, C. B. Farmer, and R. Zander, Stratospheric profiles of heavy water vapor isotopes and CH_3D from analysis of the ATMOS Spacelab 3 infrared solar spectra, *J. Geophys. Res.96,* 1057-1068, 1991.

Rothman, L. S., et al., The HITRAN92 molecular database editions of 1991 and 1992, *J. Quant. Spectrosc. Radiat. Transfer, 48,* 469-507 1992.

Schueler, B., J. Morton, and K. Mauersberger, Measurement of isotopic abundances in collected stratospheric ozone samples, *Geophys. Res. Lett.17,* 1295-1298, 1990.

Smith, R. B., Deuterium in North Atlantic storm tops, *J. Atmos. Sci., 49,* 2041-2057, 1992.

Thiemens, M. H., Mass-independent isotope effects in planetary atmospheres and the early solar system, *Science, 283,* 341-345, 1999.

Toon, G. C., The JPL MkIV interferometer, *Opt. Photonic News, 2,* 19-21, 1991.

Toon, G. C., C. B. Farmer, P. W. Schaper, L. L. Lowes, and R. H. Norton, Composition measurements of the 1989 Arctic winter stratosphere by airborne infrared solar absorption spectroscopy, *J. Geophys. Res.97,* 7939-7961, 1992.

Toth, R. A., ν_2 band of $H_2{}^{16}O$: Line strengths and transition frequencies, *J. Opt. Soc. Am. B Opt. Phys., 8,* 2236-2255, 1991.

Toth, R. A., Transition frequencies and absolute strengths of $H_2{}^{17}O$ and $H_2{}^{18}O$ in the 6.2 μm region, *J. Opt. Soc. Am. B Opt. Phys., 9,* 462-482, 1992.

Van Hook, W. A., Vapor pressures of the isotopic waters and ices, *J. Phys. Chem., 72,* 1234-1244, 1968.

This preprint was prepared with the AGU LaTeX macros v3.1. File h2ochem formatted 2001 May 3.